Materials Advances

ROYAL SOCIETY OF CHEMISTRY

PAPER

View Article Online
View Journal | View Issue

Check for updates

Cite this: *Mater. Adv.*, 2022, 3, 5080

Electrospun hydrolyzed collagen from tanned leather shavings for bio-triboelectric nanogenerators†

Lingyan Li,[ab] Jian Zhang,[ab] Manting Wang,[ab] Jiaqi Zhang,[ab] Xiao-Fei Zeng,[ab] Jie-Xin Wang[ab] and Yuan Le*[ab]

Received 24th April 2022,
Accepted 9th May 2022

DOI: 10.1039/d2ma00457g

rsc.li/materials-advances

Triboelectric nanogenerators (TENGs) have become a research hotspot as feasible energy harvesters because they can efficiently convert mechanical energy into electrical output for energy supply, showing advantages in micro-scale energy harvesting for applications in portable devices. Herein, we employed collagen extracted from leather shavings to fabricate an all-nanofiber bio-TENG *via* a cost-effective electrospinning technique. By optimizing the spinning parameters, flexible and stretchable collagen/PVA/Ag NW composite nanofiber films were successfully fabricated. The as-prepared film exhibited remarkable antibacterial activity and biocompatibility. The designed bio-TENG, using a collagen-based film and an electrospun PVDF film as the top and bottom triboelectric layers, displayed excellent electrical output performance benefiting from the rougher surface and high porosity of the contact surface. The bio-TENG can serve as a reliable power source to drive lower-power electronics. This research provides a simple and economical strategy to utilize the waste biomaterial for the construction of the bio-TENG and proposes a promising idea in the design of mechanical energy harvesters to supply low-power devices.

Open Access Article. Published on 11 May 2022. Downloaded on 8/2/2025 9:17:41 AM.
This article is licensed under a Creative Commons Attribution-NonCommercial 3.0 Unported Licence.

1. Introduction

In recent years, with the miniaturization development of portable electronic equipment, energy utilization has been transferred from centralized to decentralized and from high quality to low quality.[1,2] In 2012, based on coupling friction electrification and electrostatic induction, Wang's group invented a TENG composed of two kinds of materials with different triboelectric polarities that can efficiently convert mechanical energy into electricity, which brings a breakthrough in the technology of energy conversion and utilization.[3–5] With the further development of materials and structural design, more and more innovative, flexible, efficient TENGs are created and utilized.[6–8]

So far, the majority of triboelectric materials have been from fossil sources, exhibiting poor degradability,[9] and poor recycling performance, which are a potential threat to the environment.[10–12] Nowadays, biomaterials, like polysaccharides, lipids and proteins, as modern green sources[13] are receiving growing interest in TENGs because of their abundant reserves,[14] green product process and excellent recyclability.[15–17] Among the various kinds of biomaterials, keratin,[18,19] silk fibroin,[20,21] gelatin[22] and other animal proteins are prone to generate inductive charge after contacting with other materials due to their rich electron-donating groups like amino and amine groups, which have great potential to become the triboelectric positive material layers of bio-TENGs.[23,24] For instance, Liu *et al.*[25] have reported a bio-TENG which leverages on the regenerated spray-coating silk-fibroin film deposited on a PET/ITO substrate, exhibiting a maximum voltage of 213.9 V with a 4×6 cm^2 contact area and a high power density of 68 mW m^{-2}.

Collagen is also a typical animal structural protein that provides strength and elasticity to native tissue.[26] It is generally agreed that collagen has unparalleled biocompatibility compared with other synthetic materials.[27,28] In tannery production, more than 80% of the solid waste is composed of shaving and trimming waste,[29] which is mainly landfilled, stacked or used to produce low value-added recycled leather. With over 90% content of collagen,[30] these waste shavings cause a huge waste of biological resources.[31] Recycling of tanning waste is significant for environmental protection and sustainable development. Benefiting from rich charged amino acid residues of collagen in leather shavings, we firstly proposed to use it as a triboelectric positive material for a bio-TENG.

Meanwhile, triboelectric layers would require the rational design of triboelectric materials that can induce a high surface charge density with easy fabrication procedures in practical applications.[32,33] Compared with other methods of preparing

[a] *State Key Laboratory of Organic-Inorganic Composites, Beijing University of Chemical Technology, Beijing 100029, China. E-mail: leyuan@mail.buct.edu.cn*
[b] *Research Center of the Ministry of Education for High Gravity Engineering and Technology, Beijing University of Chemical Technology, Beijing 100029, China*

† Electronic supplementary information (ESI) available. See DOI: https://doi.org/10.1039/d2ma00457g

© 2022 The Author(s). Published by the Royal Society of Chemistry

Open Access Article. Published on 11 May 2022. Downloaded on 8/2/2025 9:17:41 AM.
This article is licensed under a Creative Commons Attribution-NonCommercial 3.0 Unported Licence.

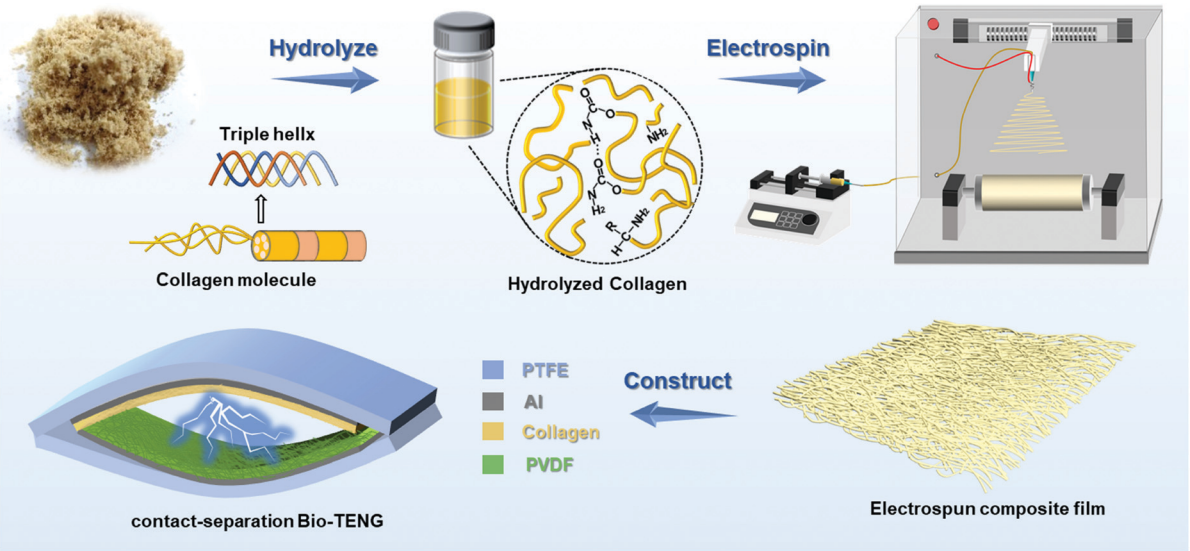

Fig. 1 Schematic illustrating the preparation process of the electrospun collagen-based composite film and the contact-separation bio-TENG.

nanofibers, like the self-assembly method and the template method,[34,35] the electrospinning technique is a more versatile and efficient technique for generating large-scale continuous fibers.[36] The chemical structure of a nanofiber film prepared by the electrospinning method is more regular under the shear force and Coulombic force generated by the high-voltage electric field, so that the electrospun films have a high crystallinity.[22,36–38] What's more, the electrospun nanofibers with a rough surface, high porosity and specific surface area offer enriched sites for capturing and maintaining large amounts of surface charge, which can greatly improve the output performance of TENGs.[32,39–42]

In this work, we presented a shaving collagen-based bio-TENG with an all-nanofiber structure produced by electrospinning technology. As shown in Fig. 1, the NaOH/urea solvent system[28,43,44] was applied to hydrolyze the waste leather shavings (glutaraldehyde tanned) to generate collagen molecules. The main electrospinning parameters were adjusted to optimize the microstructural morphologies of nanofibers and the spinning process. Conductive Ag nanowires (NWs) were innovatively incorporated into collagen-based nanofibers to serve as a triboelectric positive material. Poly(vinylidene fluoride) (PVDF) nanofiber acted as a triboelectric negative material. The antibacterial activity and biocompatibility of the electrospun membrane were evaluated. Furthermore, mechanisms of the strengthening electrical output of Ag NWs were elucidated. The prepared Bio-TENG exhibited excellent output performance, making it possible for harvesting energy and driving numerous LEDs.

2. Experimental section

2.1 Materials

The aldehyde tannage shaving waste was provided by Mingxin Xuteng New Material Co., Ltd. Sodium Dodecyl Sulfate (SDS), NaOH (AR, 96%), urea (≥99.5%), analytical reagent grade DMF, polyvinyl alcohol (PVA)-1788 and poly(vinylidene fluoride) (PVDF) powder (M_w = 400 000) were purchased from Aladdin. Ag nanowire (NW) solution (length of 10–30 μm and average diameter of 90 nm) was prepared by State Key Laboratory of Organic–Inorganic Composites. Deionized (DI) water was used in all of the experiments.

2.2 Preparation of collagen hydrolysate

The aldehyde tannage shavings waste was pretreated undergoing rinsing, filtering, drying, and grinding processes. The shavings were first cleaned in 1% SDS solution, disinfected in 75% ethanol solution, and then dispersed in ethanol with 0.5 h of stirring and 0.5 h of sonication. The resultant dispersion was filtered and placed in an oven drying at 70 °C for 4 h. After being ground, the dried shavings under 50 mesh were sifted out.

The pretreated shavings were immersed in NaOH/urea/H_2O (7 : 12 : 81, w/w/w) solution at the ratio of 1 : 20 (w/w) with stirring at 30 °C for 6–8 h. The harvested hydrolysate was thoroughly dialyzed in DI water for 2 days to remove the residual NaOH and urea. Finally, the concentrated collagen hydrolysate was obtained by reduced pressure distillation.

2.3 Preparation of collagen/PVA and collagen/PVA/Ag NWs electrospun NFs

PVA-1788 was dissolved in DI water at the concentration of 20 wt%, and then stirred for 4 h at 80 °C. A collagen/PVA spinning solution was prepared by mixing PVA aqueous solution with collagen hydrolysate at the ratio of 1 : 1 with 3 h of stirring and 0.5 h of sonication.

Meanwhile, collagen/PVA/Ag NWs spinning solutions were prepared as follows. The lab-prepared Ag NW ethylene glycol solution was washed with acetone and alcohol to remove the poly(vinyl pyrrolidone) (PVP) residue. Afterwards, Ag NWs were added to the collagen hydrolysate solution with various

Open Access Article. Published on 11 May 2022. Downloaded on 8/2/2025 9:17:41 AM.
This article is licensed under a Creative Commons Attribution-NonCommercial 3.0 Unported Licence.

concentration gradients (4 wt%, 8%, 12%, 16% and 20%) and redispersed with 0.5 h of stirring. Then, Ag NW added collagen hydrolysate and PVA precursor solutions (20 wt%) were mixed at the proportion of 1 : 1. Ultimately, homogeneous collagen/PVA/Ag NWs spinning solutions with 2 wt%, 4 wt%, 6 wt%, 8 wt% and 10 wt% Ag NWs concentrations were prepared *via* stirring for 3 h and sonicating for 0.5 h at room temperature.

In a typical fabrication procedure, the spinning solutions were placed in a plastic threaded syringe equipped with a 7-gauge metal needle. The spinning parameters were optimized in the subsequent investigations. The nanofibers were continuously collected on an aluminum foil-covered roller 18 cm distance away from the spinneret.

2.4 Preparation of PVDF electrospun NFs

The homogeneous solution of PVDF/DMF with a concentration of 16 wt% was prepared by thoroughly stirring at 80 °C for 10 h. Then the electrospinning process was conducted with a feed rate of 1.8 mL h^{-1} at high voltage of 25 kV. The temperature and humidity were controlled at 25 ± 5 °C and 45 ± 5%. The electrospun PVDF nanofibers were also collected on aluminum foils with the nozzle–collector distance fixed at 20 cm. Finally, the as-prepared samples were placed in a vacuum oven under 70 °C for 3 h to remove the residual solvent.

2.5 Preparation of the bio-TENG

The bio-TENG consists of a collagen-based electrospun film, PVDF electrospun film and aluminum foil as electrodes. The copper wire was stuck to aluminum foil layers by a copper tape for conductive connection. After that, the above-mentioned triboelectric layers were adhered to a vaulted polytetrafluoroethylene (PTFE) film of 0.5 mm thickness with great elasticity and flexibility by double-sided adhesive tape. The bio-TENG in a contact separation mode was finally obtained.

2.6 Characterization

The surface morphology and elemental component of composite nanofibers were characterized by the JSM-7800F field-emission SEM equipped with EDX. Fourier transform infrared (FTIR) spectra were measured by a Bruker Vector-70v FTIR spectrometer. TEM images of the collagen/PVA/Ag NW nanofibers were observed using a Hitachi HT-7700 transmission electron microscope. The surface roughness of the electrospun nanofibers was measured by Bruker AFM. The thermal stability of the nanofiber films was performed by thermogravimetric analysis (Netzsch). Mechanical tensile behaviors were conducted using a CMT 6503 universal tester. The periodical contact and separation of TENG was realized by a linear mechanical motor. The output electrical characteristics, including open-circuit voltage, short-circuit current, and transferred charges, were measured on a programmable electrometer (Keithley-6514), with the software platform constructed on the basis of Kickstart.

3. Results and discussion

3.1 Structural design and morphological characterization

The collagen bio-TENG in a contact separation mode held a multilayered structure made up of nanofibrous films. The positive material layers were made up of collagen-based nanofiber films. PVDF electrospun film was selected as the negative

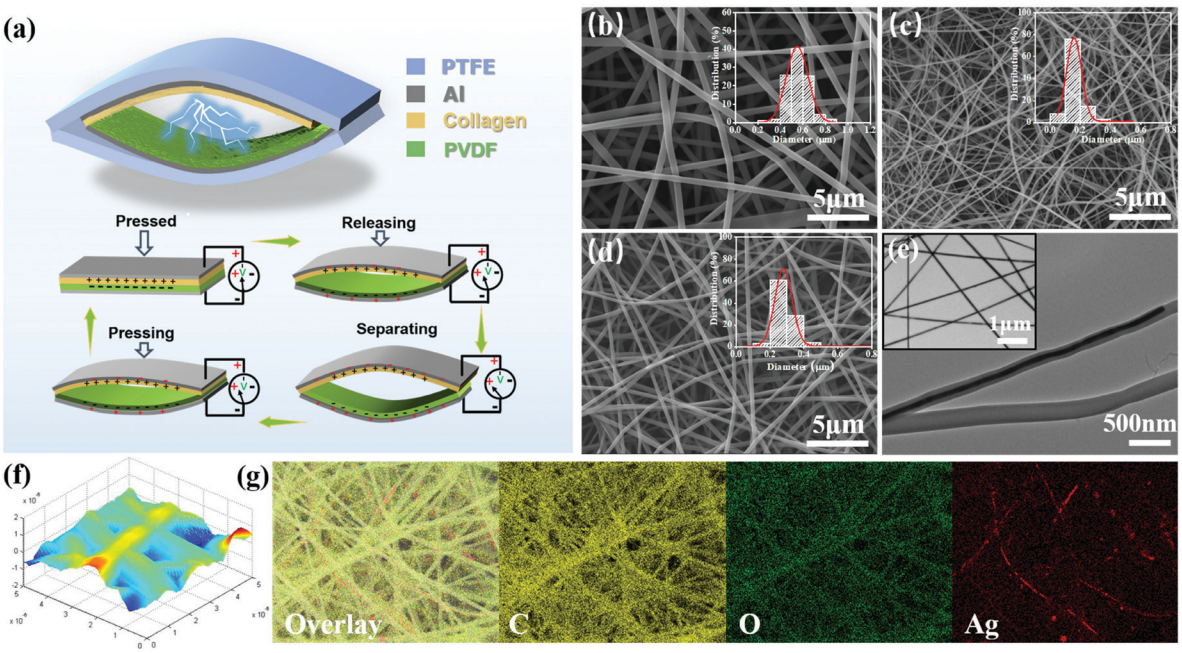

Fig. 2 (a) Schematic illustrations of the all-nanofiber bio-TENG and the triboelectric electric energy generation process. SEM images of optimized (b) collagen/PVA, (c) PVDF and (d) collagen/PVA/Ag NWs composite nanofibers with histograms of diameter distribution shown in the upper right. (e) TEM images with Ag NWs in the upper left, (f) AFM image and (g) EDX elemental mappings of collagen/PVA/Ag NWs electrospun film.

© 2022 The Author(s). Published by the Royal Society of Chemistry

Open Access Article. Published on 11 May 2022. Downloaded on 8/2/2025 9:17:41 AM.
This article is licensed under a Creative Commons Attribution-NonCommercial 3.0 Unported Licence.

triboelectric layer due to its strong electronegativity. Using aluminum foil as electrodes, the positive and negative triboelectric layers were separately adhered to an elastic and flexible PTFE vaulted film. As schematically shown in Fig. 2a, the electron transfer was realized through the periodic contact and separation motion based on the principle of coupling friction electrification and electrostatic induction.[20,45] When collagen-based layers and PVDF layers were pressed together, the positive and negative electric charges were severally gathered on the surface of two films and kept for hours. But they were confined on the surface and opposite charges coincided on almost the same plane, hardly generating an electric potential difference between the two electrodes. As contact surfaces were releasing and separating from each other, a potential difference between the layers drove electrons from the aluminum electrode of the PVDF to another, thereby forming an electric current.

As prepared by electrospinning strategy, it's important to realize the continuous spinning of hydrolyzed collagen solution and obtain membranes with a certain thickness. After being hydrolyzed by the NaOH/urea solvent system, the leather collagen had almost lost its triple-helical structure, and a large proportion of the products were in the form of hydrolyzed collagen with a simple primary structure and free amino acids (Fig. S1, ESI†). In order to improve spinnability of hydrolyzed collagen, PVA was used as an additive to increase the viscosity of the spinning solution and the strength of fiber membranes.[46] In Fig. S2–S5 (ESI†), the main electrospinning parameters such as solution concentrations, voltages, and feeding rates had been carefully adjusted with the optimum ranges of 10–12 wt% of PVA, 18–20 kV, 0.3–0.9 mL h^{-1} and no more than 10 wt% of Ag NWs. Fig. 2(b and c) exhibited SEM images of optimized collagen/PVA composite electrospun nanofibers (2b) and PVDF electrospun nanofibers (2c), the insets of which were the histograms of diameter distribution. It can be seen that the surfaces of collagen/PVA composite fibers were smooth and morphologies were uniform, in which their corresponding average fiber diameters were 500 nm and 700 nm. By contrast, the composite nanofibers with Ag NW addition had the average fiber diameters of 200 nm to 400 nm in Fig. 2d. The electrical conductivity of solution was enhanced by decorating Ag NWs so the charge density increased on the surface of the droplet and it could be stretched into thinner fibers by a greater electric field force. Fig. 2e illustrated the TEM images of nanofibers with the Ag NWs embedded forming a coaxial structure. From the elemental distribution mapping shown in Fig. 2g, it can be seen that carbon and oxygen, the main ingredients in hybrid fibers, form clear fiber outlines. The Ag element distributed parallel to the long axial direction of fibers without obvious aggregation, which suggested that Ag NWs were successfully electrospun into the collagen/PVA matrix. The 3D surface morphology from atomic force microscopy (AFM) of the nanofiber films was exhibited in Fig. 2f, showing that there were obvious height fluctuations at the location of fibers. The rougher surface increases the total effective film area so that it will display a better output performance compared with smoother films.

3.2 Nanofiber film composition characterization and properties

The composition characterization and relevant properties of different electrospun collagen-based films were compared and exhibited in Fig. 3(a–f). XRD analysis in Fig. 3a showed the diffraction peaks that occur at 2θ of 37.8°, 44.2°, 64.5°, 77.5° and 81.5° respectively corresponded to (111), (200), (220), (311), and (222) planes of the fcc structured Ag,[41] which proved Ag element existed in collagen/PVA/Ag NWs electrospun films. FTIR analysis illustrated various amide bonds of composite fibers, indicating that the chemical structures of collagen

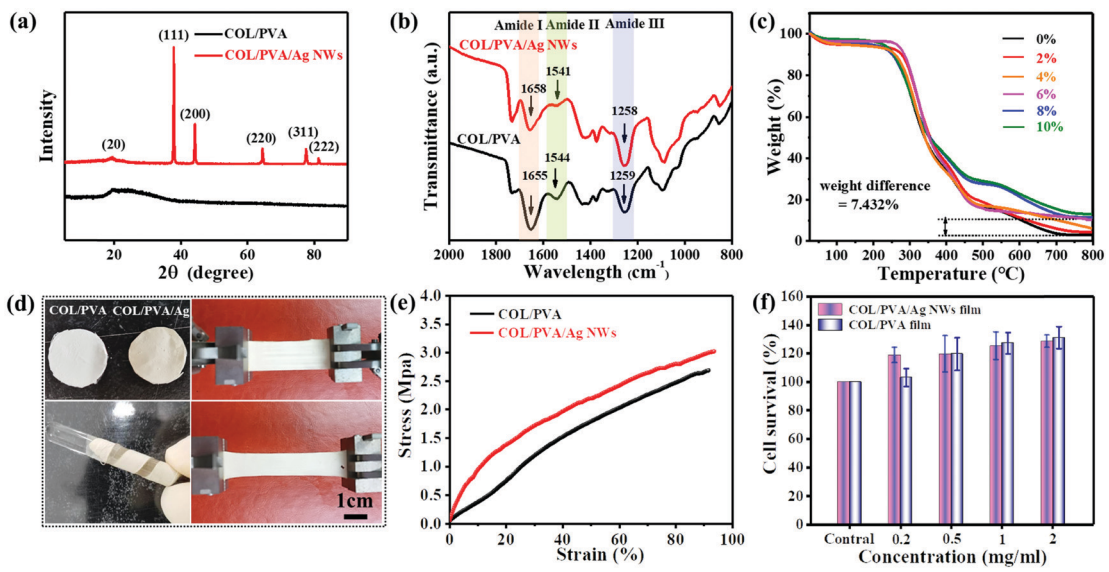

Fig. 3 (a) XRD (b) FTIR and (c) TG analyses of collagen/PVA composite film and collagen/PVA/Ag NW film. (d) Photograph images of the eletrospun nanofiber films and exhibition of stretchability, and (e) stress–strain curve from tensile tests. (f) Cell viability of different concentrations of two films.

Open Access Article. Published on 11 May 2022. Downloaded on 8/2/2025 9:17:41 AM. This article is licensed under a Creative Commons Attribution-NonCommercial 3.0 Unported Licence.

weren't destroyed in the high-voltage electric field (Fig. 3b). The actual added content of Ag NWs can be roughly estimated by the weight difference at termination point through TG analysis (Fig. 3c). Taking 8% addition as an example, the actual Ag weight content was 7.432%, which was approximately in compliance with the original addition and the same went for other groups. As can be seen in Fig. 3d, the prepared fiber film can be casually wrapped around a glass rod, indicating its excellent flexibility. The nanofiber film with a thickness of around 0.15 mm was stretched to over 90% strain level with an tensile strength of 3 MPa evaluated by tensile tests (Fig. 3e), providing good stretchability and excellent mechanical properties.

Embryonic skin fibroblast (ESF) cells were cultured in collagen composite film extract for cytocompatibility assessments by cell counting kit-8 (CCK-8) assay. As shown in Fig. 3f, hydrolyzed collagen molecules significantly increased the cell viability so there was over 20% cell proliferation compared to controls after 48 h, which confirmed the biological safety of the collagen derived from glutaraldehyde (GA) tanned leather. Besides, effects on cytotoxicity of the incorporation of Ag NWs into the composite film were negligible. The colony count method was used to evaluate the collagen/PVA/Ag NW composite film's antibacterial performance. There was an obvious decrease of residual colonies of *Staphylococcus aureus* and *Escherichia coli* on the agar Petri dish compared to the control group, and bacteriostasis rates increased with composite concentration (Fig. S6, ESI†).

3.3 Electrical output performance

For triboelectric nanogenerators, the first concern is their electrical output performance, which mainly involves open-circuit voltage (VOC), short-circuit current (ISC), and charge transfer (QSC). The factors of VOC including contact areas, frequencies and content of Ag NWs in triboelectric positive layers were explored as follows. When the contact areas of collagen/PVA TENG were changing from 1 cm^2 to 9 cm^2, the corresponding voltage increased from 31.5 V to 194 V as shown in Fig. 4a, from which it can be expected that the electrical output will increase with a larger area of the TENG. Obviously, loading frequencies ranged from 1 to 6 Hz hardly influenced the VOC (Fig. 4b). With results shown in Fig. 4c, VOC firstly increased with content of Ag NWs. However, when Ag NWs were continuously added, the VOC decreased, and the peak reached 118 V at the Ag content of 8%. At the same time, QSC increased with the increasing content of Ag NWs at first and then decreased when Ag NWs were continuously added. The peak reached 52 nC at the Ag content of 8%, which was similar to the changing trend of VOC. It can be explained that the existence of Ag NWs reduced the effective thickness of the composite membrane, thereby increasing the equivalent capacitance of

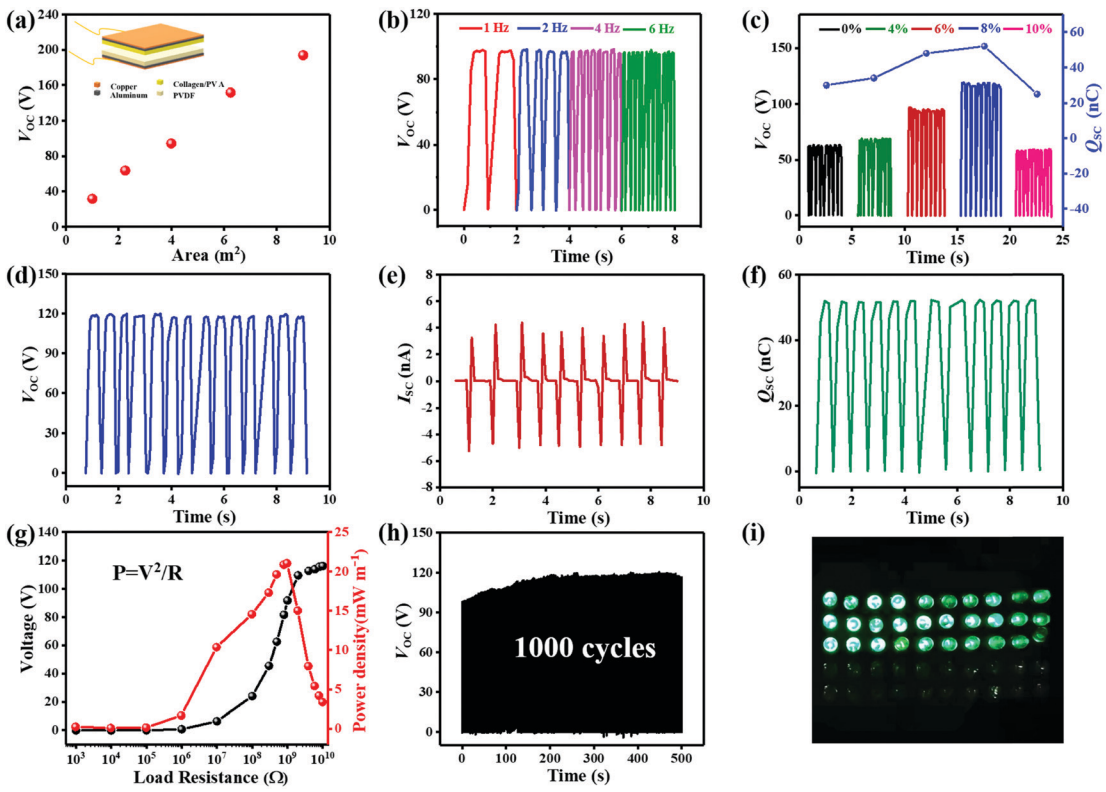

Fig. 4 The output voltage with different (a) contact areas, (b) frequencies and (c) content of Ag NWs in triboelectric positive layers. The typical electrical output performance (d) open-circuit voltage, (e) transferred charges, and (f) short-circuit current of collagen/PVA/Ag NWs TENG (2 × 2 cm^2). (g) Output voltage and power density under varied external resistances. (h) The durability test of collagen/PVA/Ag NWs TENG (2 × 2 cm^2), (i) TENG as a direct power source to light up 30 LEDs.

© 2022 The Author(s). Published by the Royal Society of Chemistry

Open Access Article. Published on 11 May 2022. Downloaded on 8/2/2025 9:17:41 AM.
This article is licensed under a Creative Commons Attribution-NonCommercial 3.0 Unported Licence.

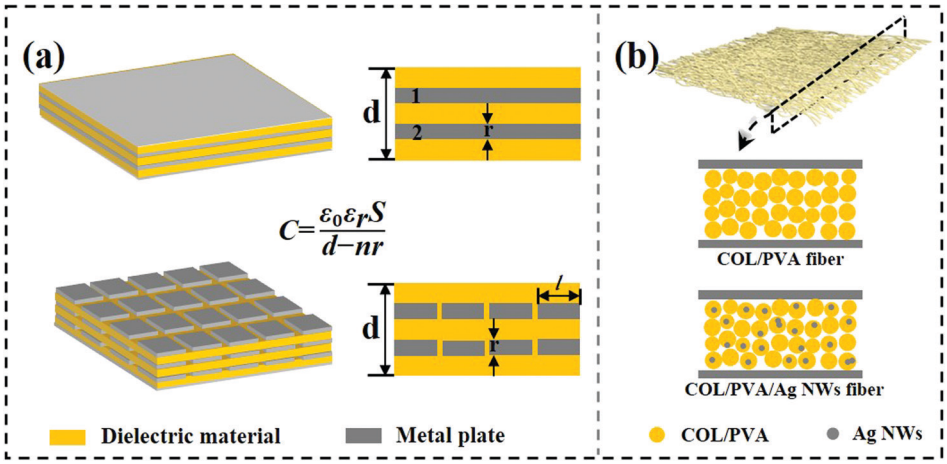

Fig. 5 (a) Schematic diagram of the capacitor structure with metal materials added. (b) Similar model of adding conductive Ag NWs into nanofibers.

the triboelectric layer to store more energy and increased the electrical output. The specific mechanism is shown in Fig. 5a. Based on electromagnetism, when n pieces of the same metal plates are inserted into a dielectric material, the equivalent capacitance is

$$C = \frac{\varepsilon_0\varepsilon_r S}{d-nr} \quad (1)$$

where ε_0, ε_r, S, d and r are the vacuum permittivity, relative permittivity, electrode surface, thickness of the dielectric film and metal plates, respectively. Then if m pieces of small plates with the area of A (a constant) are inserted in one layer and repeat for n layers, the equivalent capacitance is

$$C = \frac{\varepsilon_0\varepsilon_r mA}{d-nr} + \frac{\varepsilon_0\varepsilon_r(S-mA)}{d} = \frac{\varepsilon_0\varepsilon_r S}{d} + \varepsilon_0\varepsilon_r mA\left(\frac{1}{d-nr} - \frac{1}{d}\right) \quad (2)$$

So C increases with the growth of m and n.[47] Consequently, adding conductive Ag nanowires into nanofibers is equivalent to inserting small metal plates in dielectric materials (Fig. 5b), so that reduces the distance between the plates of the equivalent capacitor and enhances the capacitance and energy storage. However, it's worth noting that energy loss would also occur in the metals as the electric field force does work on the free electrons. Therefore, the concentration of conductive nanowires should be in a reasonable range. The typical electrical output performance of the collagen/PVA/Ag NWs TENG is shown in Fig. 4(d–f). It can deliver VOC and ISC output up to 118 V and 3.8 nA with a real contact area of 2 × 2 cm^2 under an external force. And the transferred charges achieved 52 nC per cycle.

In addition, the effective electric output of collagen bio-TENG was further measured by connecting a series of external load resistances. Fig. 4g exhibited the changing trend of output voltage and power, where the output voltage increased rapidly first and then became saturated with the load resistance from 1000 Ω to 2 GΩ. The maximum output instantaneous power reached 21.06 mW m^{-2} at the load resistance of approximately 1 GΩ, which was capable of driving some small electronic devices. Moreover, the output voltage kept stable without noticeable decay after continuous operation of 1000 cycles under an external force, which exhibited great durability of the constructed collagen bio-TENG (Fig. 4h). In the end, 30 green LEDs of 3.2 V connected in series were lit up with a contact area of 2 × 2 cm^2 as shown in Fig. 4i. Besides, it can also steadily run an electronic calculator which validated the feasibility of the TENG as a direct power source for electronics (Fig. S7, ESI†).

4. Conclusions

In summary, we present an all-fiber bio-TENG in the contact–separation mode using electrospun collagen/PVA/Ag NWs and PVDF film as the triboelectric layers. This work features the use of shavings waste for hydrolyzed collagen that can be fabricated with networked structure by using a cost-effective electrospinning technique. Addition of Ag NWs into hydrolyzed collagen from leather shavings increases both antibacterial ability and electrical output. The bio-TENG can deliver the maximum output voltage, current and instantaneous power up to 118 V, 3.8 nA and 21.06 mW m^{-2} with a contact area of 2 × 2 cm^2, which can serve as a reliable power source to drive small electronics. This research opens a simple and economical avenue to use the waste bio-material for the development of advanced eco-friendly bio-TENG for power supply and mechanical energy harvesting applications of low-power devices.

Conflicts of interest

The authors declare no competing financial interest.

Acknowledgements

This work was supported by the National Key Research and Development Program of China (2021YFA1201304 and 2021YFA1201301).

Open Access Article. Published on 11 May 2022. Downloaded on 8/2/2025 9:17:41 AM. This article is licensed under a Creative Commons Attribution-NonCommercial 3.0 Unported Licence.

References

1 Z. L. Wang and W. Wu, *Angew. Chem., Int. Ed.*, 2012, **51**, 11700–11721.
2 Z. L. Wang, *ACS Nano*, 2013, **7**, 9533–9557.
3 F.-R. Fan, Z.-Q. Tian and Z. Lin Wang, *Nano Energy*, 2012, **1**, 328–334.
4 X. Cao, Y. Jie, N. Wang and Z. L. Wang, *Adv. Energy Mater.*, 2016, **6**, 1600665.
5 H. T. Baytekin, A. Z. Patashinski, M. Branicki, B. Baytekin, S. Soh and B. A. Grzybowski, *Science*, 2011, **333**, 308–312.
6 Y. Zou, P. Tan, B. Shi, H. Ouyang, D. Jiang, Z. Liu, H. Li, M. Yu, C. Wang, X. Qu, L. Zhao, Y. Fan, Z. L. Wang and Z. Li, *Nat. Commun.*, 2019, **10**, 2695.
7 Y. Zou, L. Bo and Z. Li, *Fundam. Res.*, 2021, **1**, 364–382.
8 Y.-L. Chen, D. Liu, S. Wang, Y.-F. Li and X.-S. Zhang, *Nano Energy*, 2019, **64**, 103911.
9 Q. Zheng, Y. Zou, Y. Zhang, Z. Liu, B. Shi, X. Wang, Y. Jin, H. Ouyang, Z. li and Z. L. Wang, *Sci. Adv.*, 2016, **2**(3), e1501478.
10 A. Yu, Y. Zhu, W. Wang and J. Zhai, *Adv. Funct. Mater.*, 2019, **29**, 1900098.
11 S. Li, Y. Wang, W. Xu and B. Shi, *ACS Sustainable Chem. Eng.*, 2020, **8**, 5091–5099.
12 Z. Li, H. Feng, Q. Zheng, H. Li, C. Zhao, H. Ouyang, S. Noreen, M. Yu, F. Su, R. Liu, L. Li, Z. L. Wang and Z. Li, *Nano Energy*, 2018, **54**, 390–399.
13 Q. Liang, Q. Zhang, X. Yan, X. Liao, L. Han, F. Yi, M. Ma and Y. Zhang, *Adv. Mater.*, 2017, **29**, 1604961.
14 U. De Corato, I. De Bari, E. Viola and M. Pugliese, *Renewable Sustainable Energy Rev.*, 2018, **88**, 326–346.
15 X. Li, C. Jiang, Y. Ying and J. Ping, *Adv. Energy Mater.*, 2020, **10**, 2002001.
16 L. Cao, X. Qiu, Q. Jiao, P. Zhao, J. Li and Y. Wei, *Int. J. Biol. Macromol.*, 2021, **173**, 225–243.
17 Y. Y. Ba, J. F. Bao, H. T. Deng, Z. Y. Wang, X. W. Li, T. Gong, W. Huang and X. S. Zhang, *ACS Appl. Mater. Interfaces*, 2020, **12**, 42859–42867.
18 H. Li, T. K. Sinha, J. Lee, J. S. Oh, Y. Ahn and J. K. Kim, *Adv. Mater. Interfaces*, 2018, **5**, 1800635.
19 J. Kan, W. Li, R. Qing, F. Gao, Y. Wang, L. Zhu, B. Wang and S. Hao, *Chem. Mater.*, 2020, **32**, 3122–3133.
20 H.-J. Kim, J.-H. Kim, K.-W. Jun, J.-H. Kim, W.-C. Seung, O. H. Kwon, J.-Y. Park, S.-W. Kim and I.-K. Oh, *Adv. Energy Mater.*, 2016, **6**, 1502329.
21 D.-L. Wen, Y.-X. Pang, P. Huang, Y.-L. Wang, X.-R. Zhang, H.-T. Deng and X.-S. Zhang, *Adv. Fiber Mater.*, 2022, DOI: **10.1007/s42765-022-00150-x**.
22 S. K. Ghosh, P. Adhikary, S. Jana, A. Biswas, V. Sencadas, S. D. Gupta, B. Tudu and D. Mandal, *Nano Energy*, 2017, **36**, 166–175.
23 T.-H. Chang, Y.-W. Peng, C.-H. Chen, T.-W. Chang, J.-M. Wu, J.-C. Hwang, J.-Y. Gan and Z.-H. Lin, *Nano Energy*, 2016, **21**, 238–246.
24 W. Jiang, H. Li, Z. Liu, Z. Li, J. Tian, B. Shi, Y. Zou, H. Ouyang, C. Zhao, L. Zhao, R. Sun, H. Zheng, Y. Fan, Z. L. Wang and Z. Li, *Adv. Mater.*, 2018, **30**, 1801895.
25 C. Liu, J. Li, L. Che, S. Chen, Z. Wang and X. Zhou, *Nano Energy*, 2017, **41**, 359–366.
26 X. Liu, M. Zheng, X. Wang, X. Luo, M. Hou and O. Yue, *ACS Biomater. Sci. Eng.*, 2020, **6**, 739–748.
27 Z. Bazrafshan and G. K. Stylios, *Int. J. Biol. Macromol.*, 2019, **129**, 693–705.
28 Y. Pei, K. E. Jordan, N. Xiang, R. N. Parker, X. Mu, L. Zhang, Z. Feng, Y. Chen, C. Li, C. Guo, K. Tang and D. L. Kaplan, *ACS Appl. Mater. Interfaces*, 2021, **13**, 3186–3198.
29 X. Wang, M. Hou, X. Liu, O. Yue and M. Zheng, *ACS Appl. Bio Mater.*, 2021, **4**, 2363–2372.
30 S. Dixit, A. Yadav, P. D. Dwivedi and M. Das, *J. Clean. Prod.*, 2015, **87**, 39–49.
31 L. Guo, T. Qiang, Y. Ma, L. Ren and C. Zhu, *ACS Sustainable Chem. Eng.*, 2021, **9**, 8393–8401.
32 S. Cheon, H. Kang, H. Kim, Y. Son, J. Y. Lee, H.-J. Shin, S.-W. Kim and J. H. Cho, *Adv. Funct. Mater.*, 2018, **28**, 1703778.
33 J.-H. Zhang and X. Hao, *Nano Energy*, 2020, **76**, 105074.
34 H. Meng and Q. Wu, *Mater. Today Chem.*, 2021, **20**, 100486.
35 H. Meng and X. Qiao, *Mater. Adv.*, 2021, **2**, 7366–7368.
36 J. Xue, T. Wu, Y. Dai and Y. Xia, *Chem. Rev.*, 2019, **119**, 5298–5415.
37 R. Pan, W. Xuan, J. Chen, S. Dong, H. Jin, X. Wang, H. Li and J. Luo, *Nano Energy*, 2018, **45**, 193–202.
38 R. Sridhar, S. Sundarrajan, J. R. Venugopal, R. Ravichandran and S. Ramakrishna, *J. Biomater. Sci., Polym. Ed.*, 2013, **24**, 365–385.
39 Z. Li, M. Zhu, J. Shen, Q. Qiu, J. Yu and B. Ding, *Adv. Funct. Mater.*, 2019, **30**, 1908411.
40 X. Peng, K. Dong, C. Ye, Y. Jiang, S. Zhai, R. Cheng, D. Liu, X. Gao, J. Wang and Z. L. Wang, *Sci. Adv.*, 2020, **6**, eaba9624.
41 Z. Zhang, Y. Wu, Z. Wang, X. Zhang, Y. Zhao and L. Sun, *Mater. Sci. Eng., C*, 2017, **78**, 706–714.
42 K. Dong, X. Peng and Z. L. Wang, *Adv. Mater.*, 2020, **32**, e1902549.
43 Y. Fang, B. Duan, A. Lu, M. Liu, H. Liu, X. Xu and L. Zhang, *Biomacromolecules*, 2015, **16**, 1410–1417.
44 J. Cai, L. Zhang, S. L. Liu, Y. T. Liu, X. J. Xu, X. M. Chen, B. Chu, X. L. Guo, J. Xu, H. Cheng, C. C. Han and S. Kuga, *Macromolecules*, 2008, **41**, 9345–9351.
45 S. Niu, S. Wang, L. Lin, Y. Liu, Y. S. Zhou, Y. Hu and Z. L. Wang, *Energy Environ. Sci.*, 2013, **6**, 3576–3583.
46 O. Sanchez-Aguinagalde, A. Lejardi, E. Meaurio, R. Hernandez, C. Mijangos and J. R. Sarasua, *Polymers*, 2021, **13**, 691.
47 X. Xia, J. Chen, H. Guo, G. Liu, D. Wei, Y. Xi, X. Wang and C. Hu, *Nano Res.*, 2016, **10**, 320–330.

© 2022 The Author(s). Published by the Royal Society of Chemistry